Biol. Cybern. 71, 1–12 (1994)

Biological Cybernetics

Synapses on axon collaterals of pyramidal cells are spaced at random intervals: a Golgi study in the mouse cerebral cortex

Bernhard Hellwig [1], Almut Schüz [1], Ad Aertsen [2]

[1] Max-Planck-Institut für biologische Kybernetik, Spemannstrasse 38, D-72076 Tübingen, Germany
[2] Institut für Neuroinformatik, Ruhr-Universität, Postfach 102148, D-44801 Bochum, Germany

Received: 6 June 1993/Accepted in revised form: 22 December 1993

Abstract. In this study we investigated the arrangement of synapses on local axon collaterals of Golgi-stained pyramidal neurons in the mouse cerebral cortex. As synaptic markers we considered axonal swellings visible at high magnification under the light microscope. Such axonal swellings coincide with synaptic boutons, as has been demonstrated in a number of combined light and electron microscopic studies. These studies also indicated that, in most cases, one bouton corresponds precisely to one synapse. Golgi-impregnated axonal trees of 20 neocortical pyramidal neurons were drawn with a camera lucida. Axonal swellings were marked on the drawings. Most swellings were 'en passant'; occasionally, they were situated at the tip of short, spine-like processes. On axon collaterals, the average interval between swellings was 4.5 μm. On the axonal main stem, the swellings were always less densely packed than on the collaterals. Statistical analysis of the spatial distribution of the swellings did not reveal any special patterns. Instead, the arrangement of swellings on individual collaterals follows a Poisson distribution. Moreover, the same holds to a large extent for the entire collection of pyramidal cell collaterals. This suggests that a single Poisson process, characterized by only one rate parameter (number of synapses per unit length), describes most of the spatial distribution of synapses along pyramidal cell collaterals. These findings do not speak in favour of a pronounced target specificity of pyramidal neurons at the synaptic level. Instead, our results support a probabilistic model of cortical connectivity.

1 Introduction

Knowledge of the spatial distribution of synapses, along both dendrites and axons, is a prerequisite for an understanding of cortical connectivity. On the *dendrites* of pyramidal neurons, it is relatively easy to estimate the arrangement of synapses: they are preferably situated on spines (e.g. White and Hersch 1981), i.e. structures which can be visualized under the light microscope. On *axons*, equally conspicuous synaptic markers are not present.

Electron microscopic pictures show, however, that the axon is dilated at the location of a synapse (an example is shown in Fig. 1). These dilations are usually referred to as 'boutons' or 'synaptic terminals' (e.g. Vrensen and De Groot 1975; Matthews et al. 1976; Blue and Parnavelas 1983). Also under the light microscope, at high magnification one can recognize swellings on Golgi-stained axons (Fig. 2). There is evidence from combined light and electron microscopic studies on cortical neurons that the boutons visualized under the electron microscope and the swellings in Golgi preparations coincide (pyramidal cells: Somogyi 1978; Schüz and Münster 1985; multipolar stellate cell: Peters and Proskauer 1980; double-bouquet cell: Somogyi and Cowey 1981; chandelier cells: Somogyi et al. 1979, 1983a). Some of these studies indicate that the majority of swellings carry one synapse only, a point which is supported by similar investigations of material stained with horseradish peroxidase (McGuire et al. 1984, 1991; Kisvárday et al. 1986; White and Keller 1987). In summary, it seems that swellings on the axon collaterals of cortical neurons are good light microscopic markers for presynaptic sites.

In the present study we investigated the distribution of swellings along local axon collaterals of Golgi-stained pyramidal neurons in the mouse cerebral cortex. The question to what degree of certainty an axonal swelling can indeed be identified with a synapse will be taken up again in the Discussion. Some of the results in this paper have been presented in abstract form (Hellwig and Schüz 1989) and in Braitenberg and Schüz (1991).

2 Materials and methods

2.1 Golgi preparations

The study was performed on the neocortex of nine adult white laboratory mice (NMRI, Kißlegg). In Golgi preparations, we investigated the local axonal trees of 20

Correspondence to: B. Hellwig

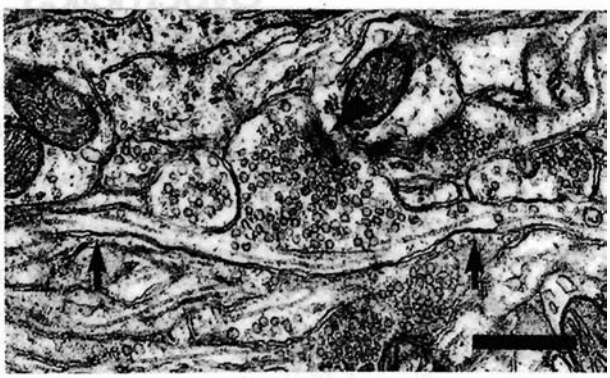

Fig. 1. Electron microscopic picture of an axon (*arrows*) which is strongly dilated at the location of a synapse (*arrowhead*). The dilation is filled with synaptic vesicles. *Bar*, 0.5 μm

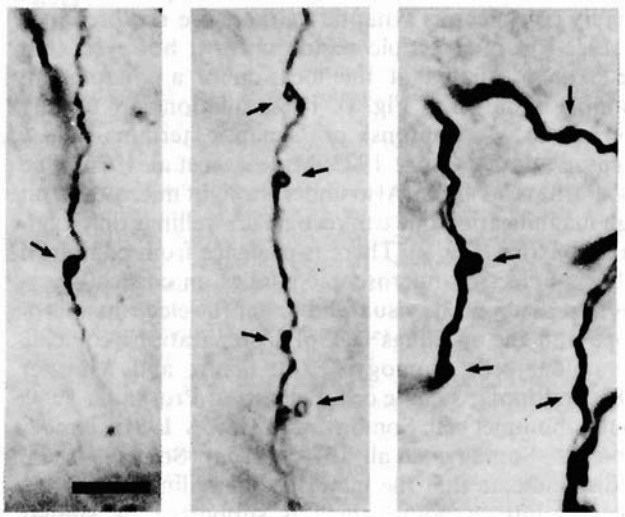

Fig. 2. Examples of axonal swellings (*arrows*) on Golgi-stained axons. *Bar*, 10 μm

pyramidal neurons. Eleven cells had been stained according to Colonnier (1964). The remaining pyramidal neurons had been impregnated by the rapid Golgi technique. Fixation had been carried out according to Peters (1970) and staining according to Valverde (1970). All brains were cut into frontal sections of about 100 μm thickness.

Neurons were selected according to the completeness and the quality of the impregnation. In addition, we required that at least some of the collaterals of each neuron have a course more or less parallel to the plane of sectioning. We did not restrict our sample of pyramidal cells to certain areas or layers of the mouse cortex. On the contrary, the neurons selected for this study were scattered over the whole extent of the neocortex (with an emphasis on its posterior parts), and they were distributed over layers II–VI. We chose this approach because we were interested in pyramidal neurons in general, i.e. in their typical features and in the variability of these features.

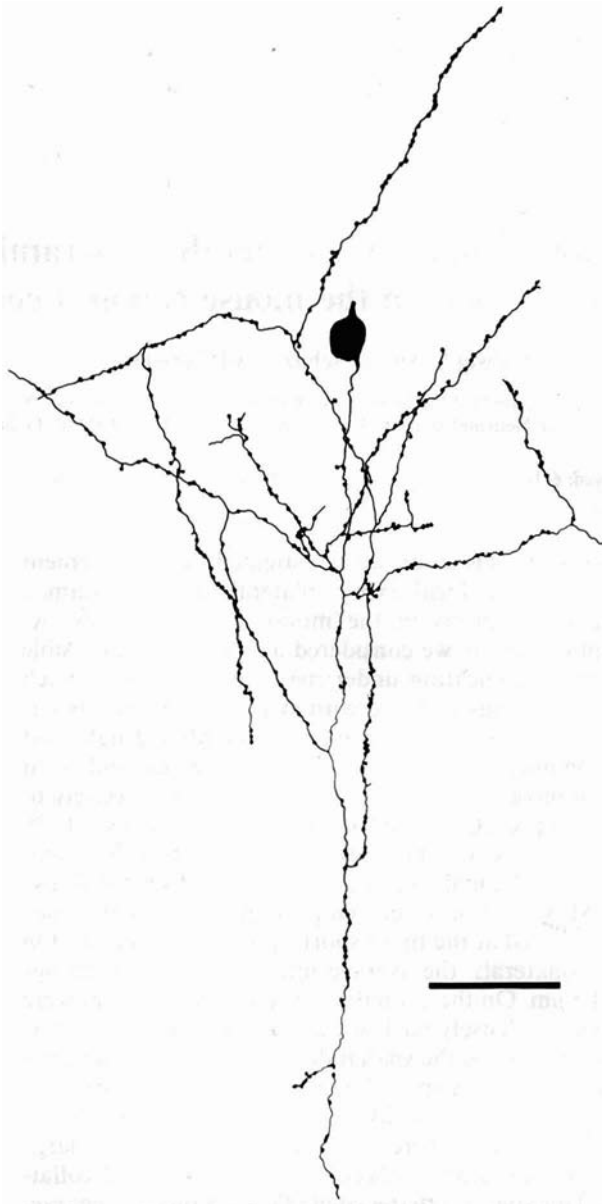

Fig. 3. Camera lucida drawing of the axonal tree of a pyramidal cell showing the distribution of axonal swellings. *Bar*, 50 μm

2.2 Quantitative analysis

Axonal arborizations were drawn with a camera lucida at a magnification of × 1000. All distinct swellings which could be recognized with the objective lens of 100/1.3 as well as the less common spine-like processes with a thickening at the tip were marked on the drawings (Fig. 3). The average distance between the marker locations was calculated by dividing the total length of the axonal ramifications of a neuron by the number of marker locations situated on them.

The length of the axonal ramifications was measured on the drawings with the aid of a Kontron Digiplan. This measurement was, however, only a first approximation since the projection of the three-dimensional axonal tree onto a two-dimensional plane by the camera lucida

shortens fibres which do not run parallel to the plane of sectioning. Using a Digimatic Indicator (Mitotoyo) fixed to the frame of the microscope, we measured the third dimension, i.e. the up or down movement of the microscope table when pursuing an axonal fibre. A better approximation to the true axonal length was then computed according to Pythagoras' theorem. Axonal fibres whose angle to the plane of projection varied along the fibre extent were subdivided into segments, and appropriate correction was applied to each individual segment.

The spatial distribution of swellings on individual axon collaterals of pyramidal cells was investigated by measuring the intervals between adjacent marker locations on the camera lucida drawings. These measurements always followed the course of the axonal fibres. In order to obtain reasonable statistics, we used only long collaterals for this purpose, i.e. fibres which were almost parallel to the plane of sectioning. Consequently, in this case no correction for shortening due to projection was made. For statistical analysis we applied standard methods from the analysis of stochastic point processes (e.g. Cox and Lewis 1966; Glaser and Ruchkin 1976).

3 Results

3.1 Density of axonal swellings

Axonal swellings were distributed over the entire axonal tree of Golgi-impregnated pyramidal neurons. Most of the swellings were 'en passant'; only occasionally were they situated at the tip of small, spine-like processes.

The total length of the axon collaterals investigated in the present study was 21 872 μm. In all, 4829 axonal swellings were counted on these fibres. This yields an average distance between swellings on axon collaterals of pyramidal cells of 4.5 μm. In individual neurons the average interval ranged between 2.4 and 7.5 μm (Fig. 4). No appreciable differences could be detected between the two Golgi procedures used: in the Golgi-Colonnier preparations the average interval between swellings was 4.7 μm (2461 swellings on a total collateral length of 11 535 μm), while with the rapid Golgi stain it was 4.4 μm (2368 swellings on a total collateral length of 10 337 μm). The scatter around these values was fairly small: in both types of preparation more than 50% of the neurons had an average interval that differed by less than 1 μm from the average value over the whole sample of neurons. On

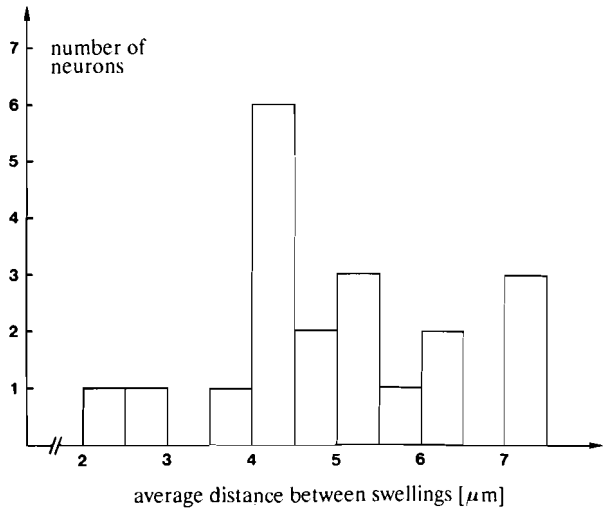

Fig. 4. Frequency distribution of the average distance between swellings on axon collaterals of pyramidal cells

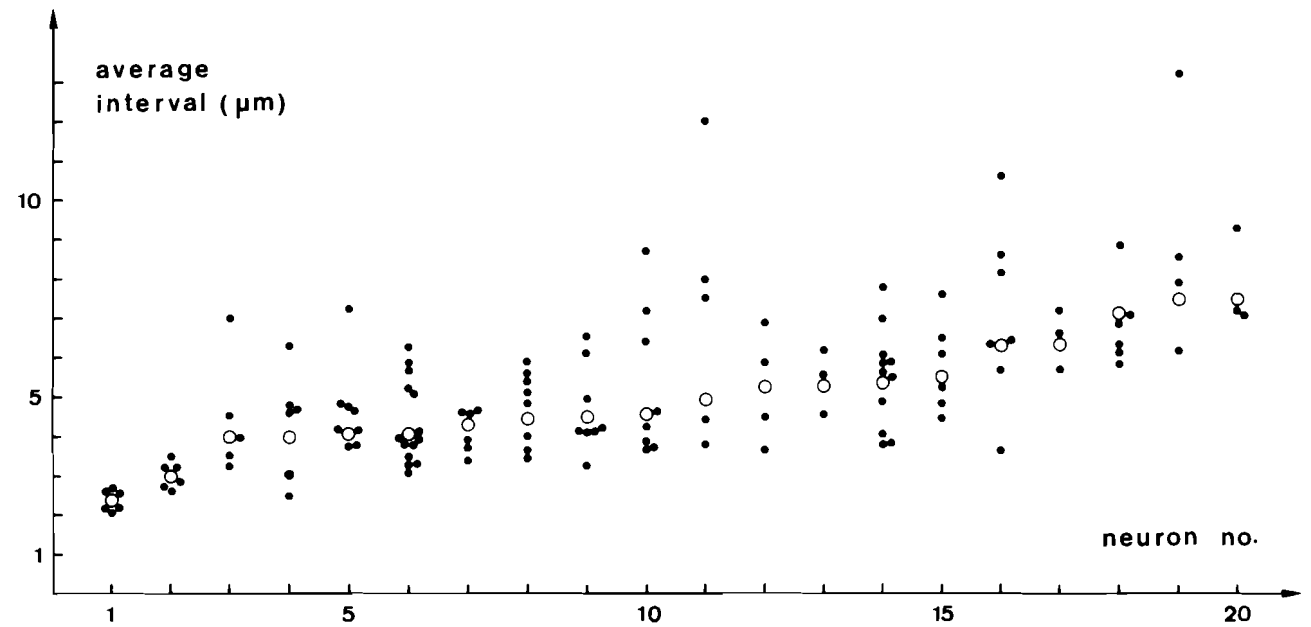

Fig. 5. Average interval between axonal swellings on individual collaterals (*filled dots*) of pyramidal cells. Only collaterals longer than 60 μm are shown. The *open circles* indicate the average for all collaterals of one neuron. The neurons are ordered along the *abscissa* according to the size of their average interval

the main axon the average distance between swellings was always clearly larger (at least by a factor of 1.6) than on the collaterals. Since the two Golgi preparations used yielded very similar results, they will not be considered separately in the following sections.

3.2 Spatial distribution of axonal swellings: deterministic or stochastic?

The intervals between swellings on the axon collaterals of pyramidal cells were investigated in more detail. First, we compared *different collaterals of the same neuron.* The diagram in Fig. 5 shows the results for collaterals longer than 60 μm. The average interval between swellings on different collaterals of the same neuron may vary by up to a factor of 3. It should be noted, however, that if only very long fibres are considered, the average values for different collaterals tend to be much more similar (cf. Fig. 12). Hence, the scatter in Fig. 5 is mainly due to the shorter collaterals, where the statistical reliability is accordingly smaller. We will return to this issue later.

Secondly, we investigated the arrangement of swellings along *individual collaterals* of pyramidal neurons. Thirty-three collaterals, i.e. all primary collaterals which were longer than 150 μm or which carried at least 30 axonal swellings, were analysed in more detail. Inspection of Fig. 6, showing the distribution of swellings on these collaterals, leads to the following impression: several collaterals show a lower density of swellings proximally (nos. 3, 20, 21), but this does not seem to be a general rule (nos. 2, 7, 8, 13). In some cases there appears to be a tendency towards clustering of swellings (nos. 4, 7, 8), in others towards more regular distances (no. 31).

In order to assess the quantitative characteristics of the underlying spatial distribution(s) of swellings, we investigated the 33 primary collaterals presented in Fig. 6 in more detail by a statistical analysis. Figure 7 shows interval distributions for the entire sample of collaterals (Fig. 7a) and for individual collaterals (Figs. 7b–e). In the

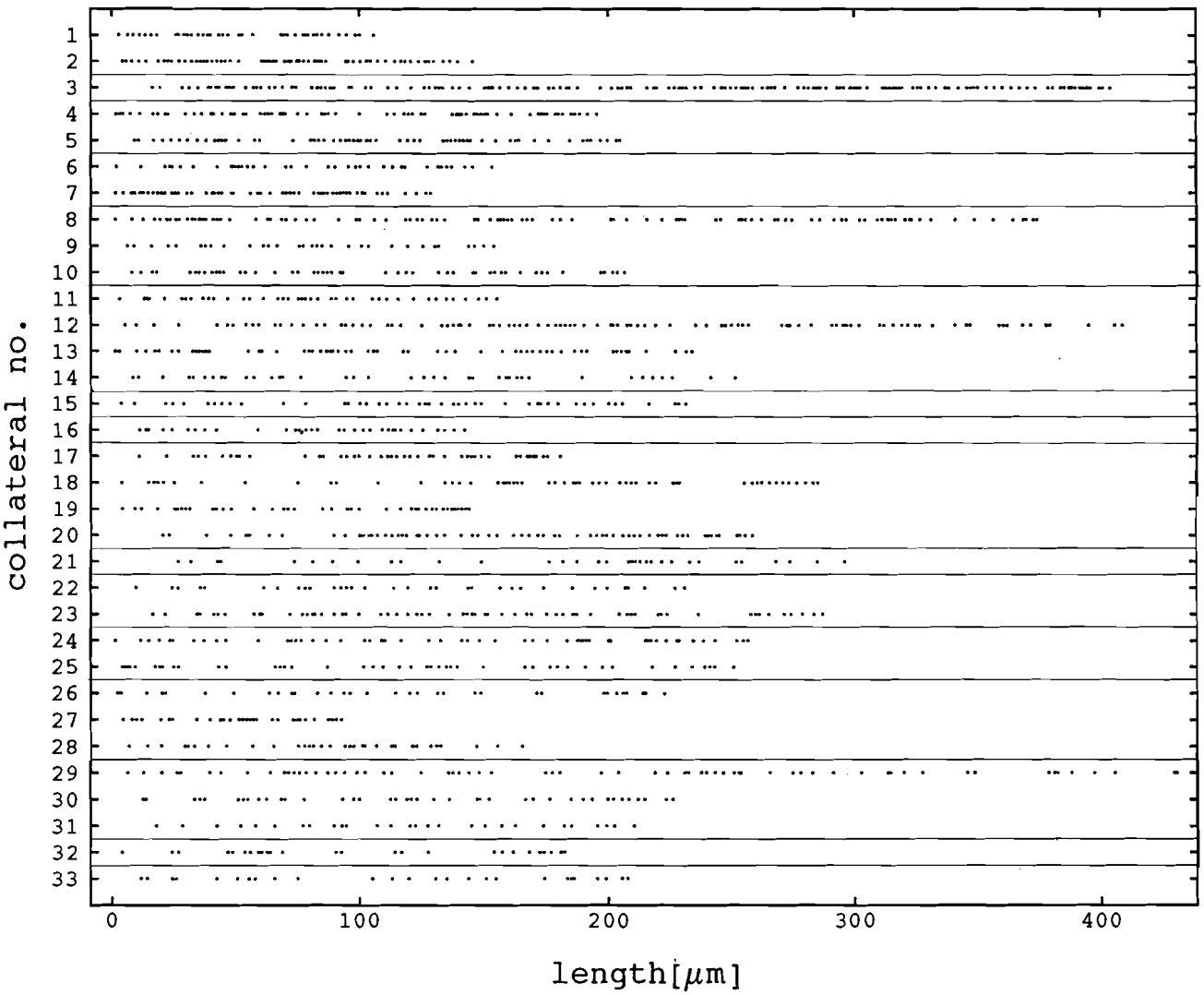

Fig. 6. Arrangement of axonal swellings on the 33 primary collaterals used for statistical analysis. Each *dot* corresponds to the location of a swelling. The origin of each collateral (the branching point from the main stem) is on the *left*. Collaterals *between adjacent horizontal lines* originate from the same neuron

latter case, results for the four longest collaterals are displayed (nos. 3, 8, 12, 29 in Fig. 6). Since they also carried the largest number of swellings (143, 98, 96 and 65 swellings, respectively), they can be considered as the statistically most reliable ones of our sample. Moreover, these four collaterals cover the spectrum of synaptic densities contained in our sample: the average interval is small on collateral no.3 (2.5 μm), it is intermediate on collaterals no. 8 (3.7 μm) and no. 12 (4.1 μm) and large on collateral no. 29 (6.2 μm). The interval histograms in Fig. 7 are highly suggestive of the exponential type. This observation is supported by plotting the histograms on a logarithmic scale (Fig. 8): the decline now approximates a straight line. Only in the case of collateral no. 29 (Figs. 7e and 8e) is an exponential decline less obvious. This can be explained by the lower number of intervals and the larger average interval between swellings, which cause the descent to be less steep. After replotting Fig. 7e with larger bins, the correspondence to an exponential distribution indeed becomes more convincing. Finally, we note that the dip in the interval distribution for very short intervals is caused by the finite extent of the swellings (diameter range up to 1 μm).

The interval distribution measures the relative frequency of intervals of different lengths, irrespective of where they occur along the collateral. Consequently, the

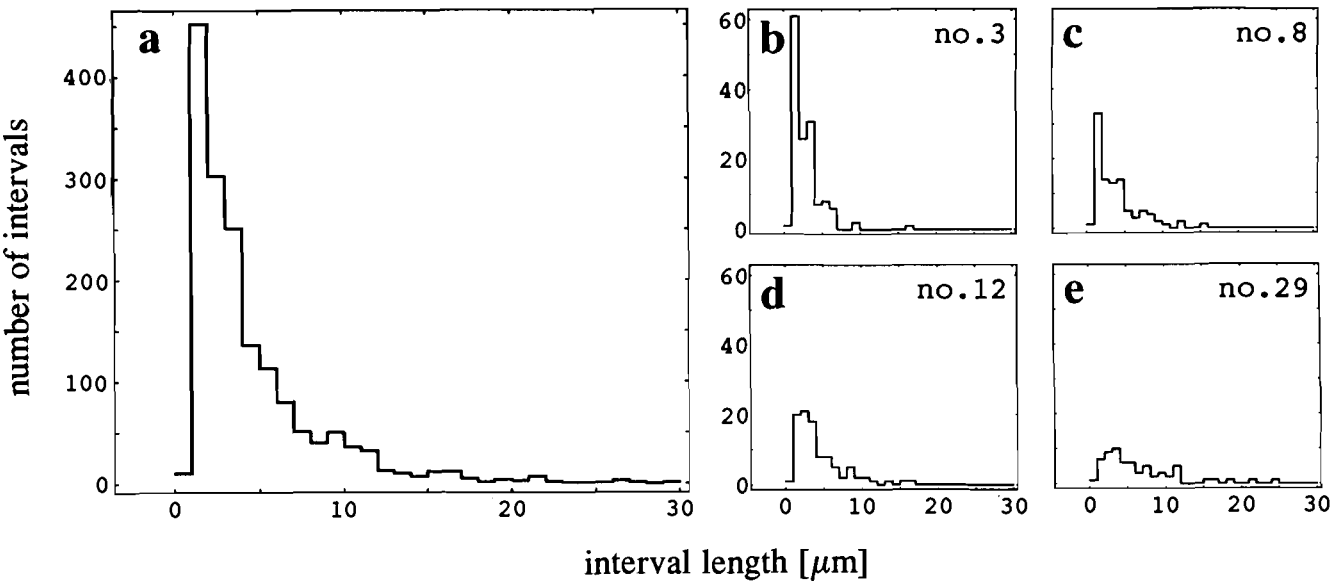

Fig. 7. Interval histograms of the entire sample of collaterals (**a**) and of the four longest collaterals (**b-e**) which also have the highest number of swellings. The *numbers in the upper right corners* in **b-e** refer to the fibre identities in Fig. 6. The average interswelling intervals for the individual collaterals are: 2.5 μm (**b**), 3.7 μm (**c**), 4.1 μm (**d**), 6.2 m (**e**)

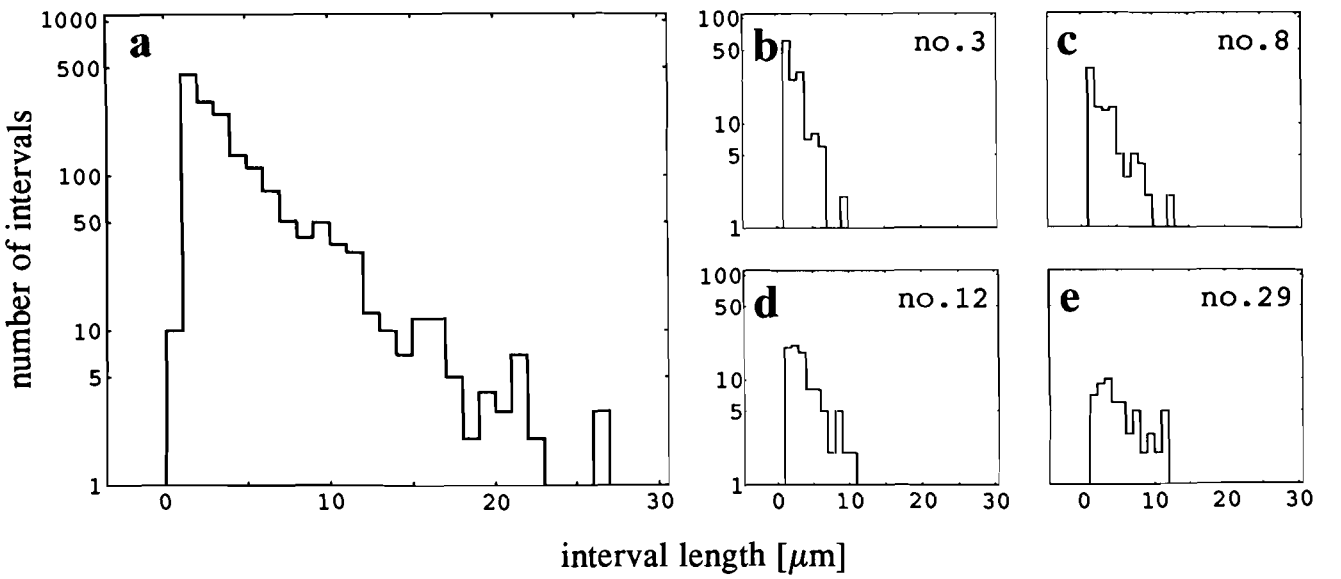

Fig. 8a–e. The interval histograms of Fig. 7 shown as logarithmic plots

interval histogram does not enable us to decide whether a relationship possibly exists between neighbouring intervals, e.g. whether swellings tend to cluster or whether smaller intervals are preferentially surrounded by larger ones. This issue can be addressed by producing a scatter diagram, in which each interval i_n is plotted against the following interval i_{n+1}. Any pattern in the distribution of swellings along the axon would show up as a characteristic pattern in such a diagram. Scatter diagrams for the whole sample of collaterals and for the four longest collaterals are displayed in Fig. 9. No distinct patterns are apparent here; this lack of neighbourhood relationship is quantified by the serial correlation coefficients having values in a narrow range around zero (cf. legend to Fig. 9). The serial correlation coefficients of higher order (up to order 5), reflecting statistical dependency between next-to-nearest neighbour intervals and so on, were also restricted to a narrow range around zero (all values were between -0.1 and $+0.1$, with two outliers at -0.11 and 0.14, respectively), thus ruling out the possibility of more complicated serial dependencies across larger stretches of axon and for larger numbers of intervals.

Finally, the autocorrelation histograms of the four longest collaterals are shown in Fig. 10. The actocorrelation function measures the probability of finding an axonal swelling as a function of the distance to any given swelling (irrespective of the number of swellings in between the two). The flat autocorrelation histograms for each of the collaterals show that this probability is uniform, i.e. independent of the distance (except of course for the trivial peak at distance 0, and the small dips surrounding the origin caused by the finite extent of the individual swellings). Note that this also holds true for collateral no. 29, for which the exponential approximation to its interval distribution (cf. Figs. 7e and 8e) remained somewhat doubtful. Note also that, in each case, the autocorrelation coincides with the value predicted on the basis of the average intervals (arrowheads in Fig. 10). This again speaks against the possibility of any dependencies over larger distances.

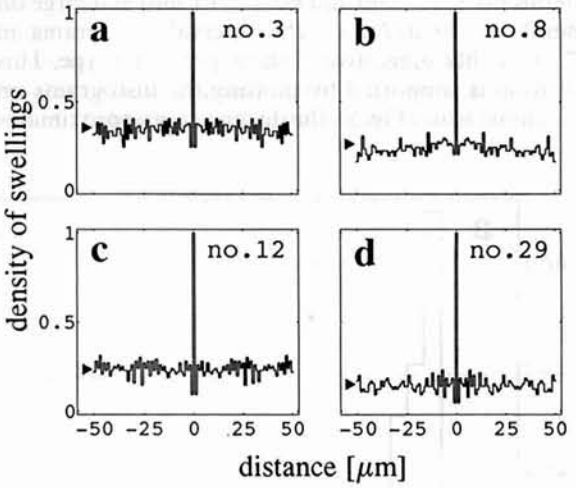

Fig. 10a–d. Autocorrelograms for the same collaterals as in Fig. 7. The *abscissa* shows distances between swellings, the *ordinate* the density of swellings per bin (bin size 1 μm). The density of swellings per bin can be interpreted as the probability of finding a swelling as a function of a certain distance to any given swelling. Apart from the trivial peak at position 0 and the small dip surrounding it, the autocorrelograms are essentially constant. Moreover, they equal the value, predicted on the basis of the average interswelling interval (*arrowheads*), which argues against the presence of any long-range trends in synaptic density along the axon collateral

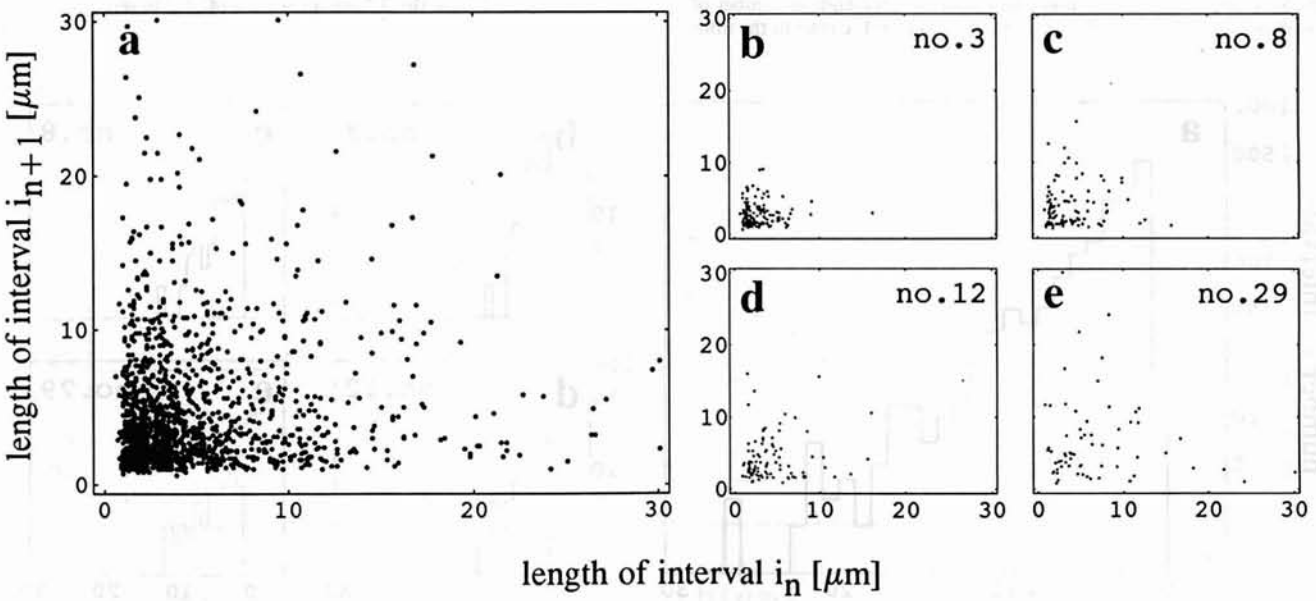

Fig. 9. Scatter plots of the whole sample of collaterals (**a**) and of the same collaterals as in Fig. 7(**b-e**). Each interval i_n is plotted against the following interval i_{n+1}. Observe that the sizes of neighbouring intervals appear to be statistically independent. This is quantified by the very low values of all serial correlation coefficients r_i up to order $i = 5$: all values are well within the range of -0.1 to $+0.1$, with the exception of two outliers ($r_2 = -0.14$ for collateral no. 3, $r_2 = +0.11$ for collateral no. 8)

Summarizing, the results of the statistical analysis presented in Figs. 7–10 suggest (1) that the intervals between neighbouring axonal swellings are drawn from an *exponential distribution*, (2) that the process governing the spatial distribution of these intervals is *renewal*, i.e. that neighbouring intervals are statistically independent, and (3) that the probability of finding an axonal swelling as a function of the distance to any given swelling is *uniform*, i.e. independent of the distance between the two. All in all, these findings indicate that the arrangement of swellings along individual collaterals of pyramidal neurons can be described by a stochastic process, which is completely specified by the rate constant of its exponential interval distribution; in other words, a Poisson process (e.g. Cox and Lewis 1966; Glaser and Ruchkin 1976).[1]

We should mention, though, that one collateral in our sample (no. 4 in Fig. 6) did not fit the simple Poisson model. The interval histogram and the scatter diagram for this collateral (Fig. 11a–c) reveal that swellings are more clustered than would be expected in the case of a true Poisson distribution. The autocorrelation histogram (Fig. 11d), however, is again essentially flat.

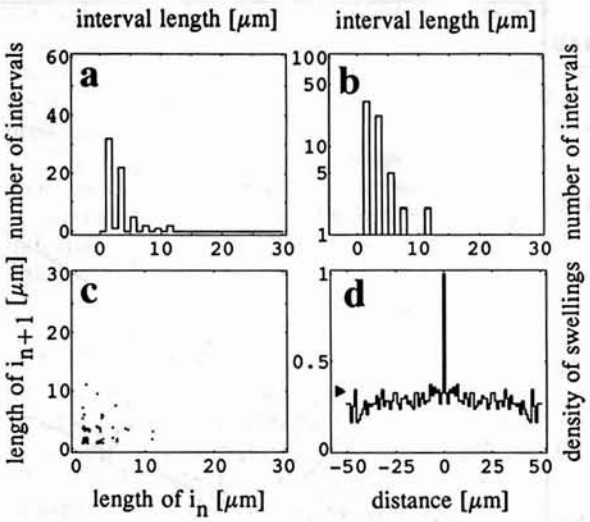

Fig. 11a–d. Statistical analysis (as in Figs. 7–10) of axon collateral no. 4 (cf. Fig. 6). This particular collateral presents an outlier in the sense that it shows distinctly more spatial structure than any of the others. This is particularly clear in the interval histogram (**a, b**) and the scatter diagram (**c**). Serial correlation coefficients are distinctly higher than for the cases in Fig. 9 ($r_1 = 0.15$, $r_2 = -0.02$, $r_3 = -0.24$, $r_4 = -0.14$, $r_5 = 0.16$). Note, however, that even in this case, the autocorrelation is essentially flat and coincides with the value predicted on the basis of the average interswelling interval. The downward tendency for larger distances in an artefact, due to the limited length of the collateral

3.3 Is there a single distribution of intervals between swellings?

In view of the statistical findings described in the previous section, the question arises as to whether the whole sample of collaterals receives its synapses from one and the same distribution of interswelling intervals, or whether one has to invoke several different distributions (all of the Poisson type, but with different rate constants). Or, if one characterizes the spatial distribution of axonal swellings metaphorically as though it had 'rained' synapses onto the axonal fibres, one might wonder whether it 'rains' with the same or with different strengths in different parts of the cortex. The latter possibility might seem plausible in view of the considerable scatter in the average intervals on different collaterals of the same neuron (cf. Fig. 5).

The scatter in Fig. 5 could, however, also have a simple statistical explanation: it might be due to the variance in the lengths of the investigated segments of collaterals. Short portions of collaterals would tend to yield lower numbers of swellings, thereby causing higher statistical variance. Figure 12 reveals that this is indeed the case. The average interval between swellings on all individual collaterals in our sample of pyramidal cells is plotted as a function of the collateral length. This length was either the true length of the collateral (if it was contained completely in the section) or – which was actually more often the case – the length of an initial segment of a collateral leaving the section. Inspection of Fig. 12 shows that the small numbers of swellings on

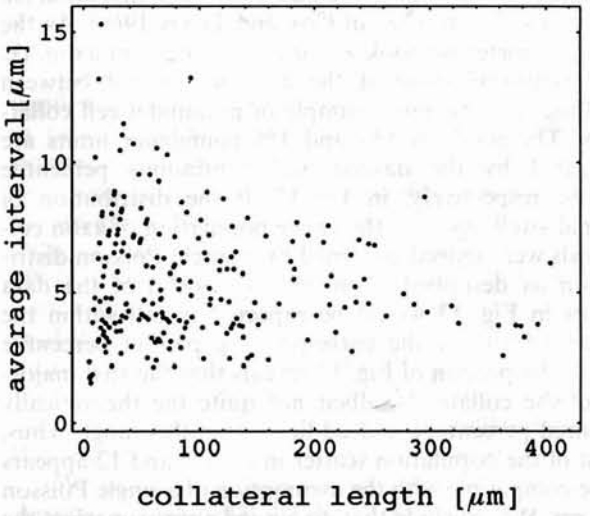

Fig. 12. For each collateral in our sample, the average interval between swellings is plotted against the collateral length. Observe that the variance of the average interval decreases with increasing collateral length

short collaterals yield strongly varying average intervals between swellings. With increasing collateral length, however, the variance of the average interswelling interval decreases considerably.

In order to test statistically whether a *single* distribution of interswelling intervals is compatible with our experimental data, we compared these with theoretical results (Fig. 13). For each collateral in our sample, the number of swellings is plotted against the collateral

[1] More precisely (also in view of the 'dead interval' caused by the finite extent of the swellings), we should, in fact, speak of discrete Bernoulli trials (Feller 1957), with the Poisson model as an appropriate and commonly used approximation

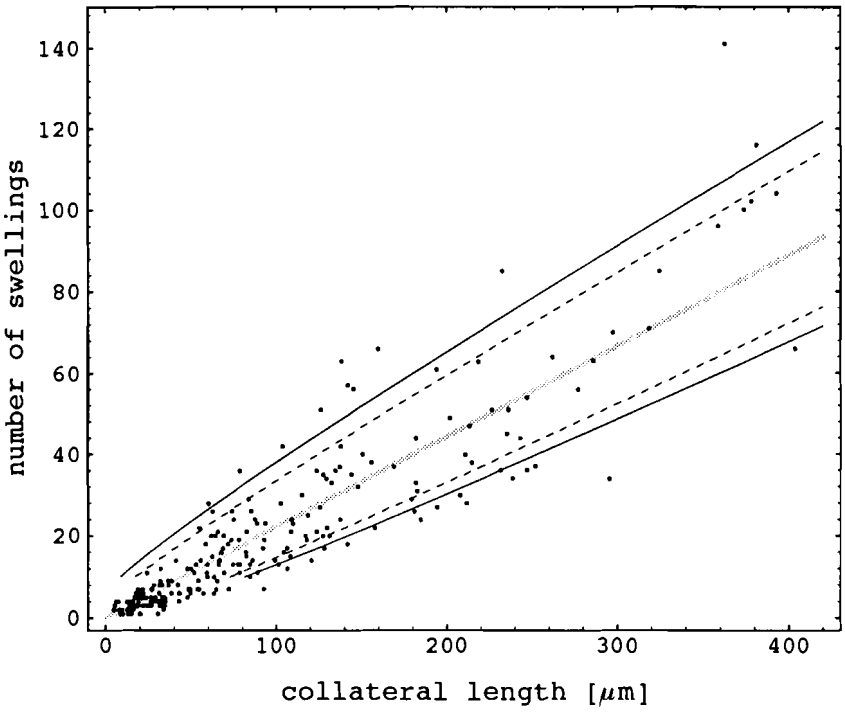

Fig. 13. For each individual collateral, the number of synaptic swellings is plotted as a function of the collateral length. If the entire population of collaterals were governed by a single Poisson process, characterized by a constant rate parameter $\lambda = 0.22$ synapses/μm axon (the reciprocal value of the average interval over the entire population), then 95% (99%) of the values should be located within the *dashed* (*continuous*) confidence limits predicted by the model. Observe that the vast majority of collaterals, albeit not quite the required percentages, indeed falls within these ranges. The confidence limits are only shown for numbers of swellings above 10; for smaller values they become discontinuous, which would clutter the already crowded picture near the origin. The *straight grey line* indicates the number of swellings expected at a certain collateral length (if a Poisson process with $\lambda = 0.22$ synapses/μm is assumed). Observe that the data points are scattered around this line, i.e. the average number of swellings increases roughly proportionally to the collateral length. Note, however, that there is a slight tendency of points to fall below the expected value for short collaterals and to fall above it for long collaterals. For further discussion, see text

length. In addition, we calculated the confidence limits for the number of swellings as a function of axonal length expected on the basis of a single Poisson distribution (cf. equations (2.6) to (2.8) in Cox and Lewis 1966). As the rate parameter we took $\lambda = 0.22$ swellings/μm axon, i.e. the reciprocal value of the average interval between swellings for the entire sample of pyramidal cell collaterals. The resulting 5% and 1% confidence limits are indicated by the dashed and continuous percentile curves, respectively, in Fig. 13. If the distribution of axonal swellings over the entire population of axon collaterals were indeed governed by a single Poisson distribution as described, then 95% (or 99%) of the data points in Fig. 13 would be expected to fall within the range defined by the corresponding pair of percentile curves. Inspection of Fig. 13 reveals that the vast majority of the collaterals, albeit not quite the theoretically required percentage, indeed lies within this range. Thus, most of the population scatter in Figs. 5 and 12 appears to be compatible with the assumption of a single Poisson process. We conclude that, to a good approximation, the spatial distribution of swellings along axon collaterals of cortical pyramidal cells is governed by a single Poisson model, characterized by its rate constant $\lambda = 0.22$ swellings/μm. Note, however, that the number of swellings in Fig. 13 tends to be slightly smaller than expected for short collaterals and somewhat larger than expected for long collaterals. In fact, for collaterals shorter than 50 μm the average density of swellings is $\lambda = 0.19$ swellings/μm; for collateral lengths between 50 and 250 μm it is $\lambda = 0.22$ swellings/μm; and for collaterals longer than 250 μm it is $\lambda = 0.24$ swellings/μm. Thus, the overall rate λ of the Poisson process might, in fact, slightly increase with increasing collateral length. This is, of course, only true if the 'short' collaterals in our sample are really short. Many of them, however, may well be the initial segments of long collaterals leaving the section. In that case it is conceivable that the rate λ of the Poisson process depends on the distance from the proximal branching point of the collateral, with λ slowly increasing as one proceeds along the collateral. Such a Poisson process is commonly referred to as 'inhomogeneous' or 'rate-modulated' (e.g. Cox and Lewis 1966).

4 Discussion

4.1 Relationship between axonal swellings and synapses

The question to what extent the axonal swellings observed in Golgi preparations can be identified with synapses can be decomposed into three more specific questions.

1. How often does an axonal swelling carry more than one synapse? Combined light and electron microscopic studies indicate that 1–3% of the axonal swellings on pyramidal cell axons carry more than one synapse (Winfield et al. 1981; McGuire et al. 1984, 1991; Kisvárday et al. 1986). In one case, a higher percentage (19%) was found (Schüz and Münster 1985). On axons of nonpyramidal neurons, values of 7% (DeFelipe and Fairén 1988) and 11% (Somogyi et al. 1983b) have been reported. In a somewhat different approach, using conventional electron microscopic material of the mouse cortex, we also found a low percentage of boutons (8.6%) carrying more than one synapse (Hellwig 1992). In this study serial sections of 35 boutons forming synapses of the asymmetric type were examined. Although one cannot exclude that some of these boutons were of extracortical origin (Peters and Feldman 1976), most of them can be

assumed to belong to axons of pyramidal cells including spiny stellates (Peters and Jones 1984).

2. Are synapses exclusively located on axonal swellings? All of the 151 synapses investigated in a combined light and electron microscopic study by McGuire et al. (1984) were located on axonal swellings. In a study by Schüz and Münster (1985), one synapse out of 28 could not conclusively be associated with a swelling visible under the light microscope. To our knowledge, no other reports of synapses located outside axonal swellings exist. This makes it plausible that such synapses are indeed quite rare. Our own observations (Hellwig 1992) of electron microscopic serial sections of the mouse cortex support this point: synapses were only see on distinct axonal dilations.

3. Do all axonal swellings carry a synapse? In most combined light and electron microscopic studies, there was no evidence of axonal swellings or boutons without a synapse. This was true for both pyramidal cells (Somogyi 1978; Schüz and Münster 1985; Kisvárday et al. 1986) and non-pyramidal cells (Somogyi et al. 1979, 1983a, b; Peters and Proskauer 1980; Somogyi and Cowey 1981; Freund et al. 1983; Kisvárday et al. 1987). In two studies (Winfield et al. 1981; DeFelipe and Fairén 1988), axonal dilations could not always be identified with synaptic boutons. However, in both cases the authors suggest that some synapses may have been obscured by the deposit of the Golgi stain.

To summarize, while the correspondence between axonal swellings and synapses is not exactly one-to-one, it is certainly not far removed from it. We conclude, therefore, that the spatial distribution of axonal swellings, as visualized under the light microscope, is a useful measure for the locations of presynaptic sites on axons.

4.2 Synaptic density

The density of swellings on pyramidal cell collaterals observed in the present study is in good agreement with the density of synapses found on the distal part of the axonal tree of a pyramidal neuron investigated by Schüz and Münster (1985). Moreover, in both studies swellings or synapses were found to be more densely packed on collaterals than on the main axon.

Winfield et al. (1981) reported data on a pyramidal cell in the monkey somatic sensory cortex which are at variance with our observations in three respects: (1) most of the synapses in their study were located on spine-like processes and a smaller number on 'en passant' swellings of the axon; (2) these 'spines' were more densely packed on the main axon than on the collaterals; and (3) the overall density of these axonal 'spines' was considerably lower than the density of swellings on the axonal trees in the present study. This discrepancy might reflect a difference between the species involved; in addition, as mentioned above, one cannot rule out the possibility that some synapses on swellings in the monkey pyramidal cell remained undetected because of the Golgi precipitate.

Martin and Whitteridge (1984) showed that on axons of unspecified neurons in the cat visual cortex (probably both pyramidal and non-pyramidal cells), most of the intervals between en passant swellings or spine-like processes ranged between 1 and 15 μm, with a strong tendency towards values between 1 and 3 μm. The interval histogram shown in their study is similar to the ones presented here.

The average distance between swellings does not seem to vary between cortical areas. Amir et al. (1993) showed that the median of the inter swelling intervals on biocytin-stained axonal fibres is constant at 6.4 μm in different areas of the monkey visual cortex.

4.3 Axonal length

The data on synaptic density along axon collaterals can be used to verify other statistical measures on the cortex, for example measurements of axonal length per volume. Since the average interval between swellings on axons of non-pyramidal neurons (Hellwig 1992) is similar to that presented here for pyramidal cells (4.6 μm for Martinotti cells, 5.7 μm for other non-pyramidal cells), one can assume a total average of approximately one synapse every 5 μm of axonal length. If the number of synapses in 1 mm^3 of cortex (7.2×10^8 synapses/mm^3 in the mouse; Schüz and Palm 1989) is multiplied by 5 μm, a total axonal length of 3.6 km per mm^3 of cortex is obtained. This confirms earlier estimates (1–4 km/mm^3) on the mouse cortex by Braitenberg (1978a). It is also consistent with an electron microscopy study by Foh et al. (1973), who found the length of neuronal processes (axons plus dendrites) in the visual cortex of the cat to be at least 5 km/mm^3.

The total axonal length per unit volume can also be verified by another, independent argument and can thus, in turn, be used as a countercheck of the density of synapses in the present study. One can calculate whether the axonal length per volume is compatible with what is known about the diameter of axons. Axons occupy about 29% of the cortical volume (Braitenberg and Schüz 1991). If one wishes to fit 3.6 km axon into 1 mm^3 of cortex, the average diameter must consequently not exceed 0.32 μm. This is exactly the value which has been measured by Foh et al. (1973) on electron micrographs of the cat visual cortex and is close to our measurements in the mouse cortex: 0.3 μm in Golgi preparations and 0.27 μm on electron micrographs (Schüz 1989).

We can also estimate the axonal length per neuron. Assuming a neuronal density of 9.2×10^4 neurons/mm^3 in the mouse cortex (Schüz and Palm 1989) and an axonal density of 3.6 km/mm^3, the mean axonal length per neuron turns out to be 39 mm.

4.4 Spatial distribution of synapses on pyramidal cell collaterals

The present study focuses on the local axonal tree, i.e. on that part of the axonal tree which ramifies before the main axon enters the white matter. Distant arborizations made via cortico-cortical connections could not be considered because of the limitations of the Golgi technique, which tends not to stain myelinated fibres (Ramón y Cajal 1911). One can assume, however, that the average

density of synapses on these distant ramifications does not differ too much from that on the local ones: any substantial difference should have manifested itself in the numerical countercheck between density of swellings, total axonal length per unit volume and axon diameter discussed in the previous section.

Our results indicate that the distribution of presynaptic sites on local axon collaterals of pyramidal cells is random or, to put it more precisely, that it follows a Poisson distribution, with a lower bound on the possible intersynapse intervals. In other words it appears as though it had 'rained' synapses onto the axonal fibres, or, alternatively, as though synapses had 'sprung' up regardless of the occupancy at neighbouring stretches of axon. This allows us to make some inferences regarding the connectivity of pyramidal cells in the cortex. It excludes the kind of target specificity observed in certain non-pyramidal neurons, the chandelier cells. These show a strong clustering of swellings at vertical segments of their ramifications, which are known to synapse specifically onto the axon initial segments of pyramidal cells (Somogyi et al. 1979, 1983a). In contrast, our results support the hypothesis that pyramidal cells distribute their synapses onto many thousands of different postsynaptic neighbours, without being particularly fastidious in the distribution of their 'favours' (Braitenberg 1978b). If a collateral were to strive for multiple contacts with selected dendrites, one would expect clusters of swellings beyond those predicted by a Poisson distribution. Our results show that this is not the case. However, as demonstrated by collateral no. 4 in our sample (cf. Fig. 11), there may be single collaterals which are at variance with the overall picture.

In Fig. 13 we analysed whether out experimental data were compatible with the assumption of a single distribution of interswelling intervals, or whether several different distributions (all of the Poisson type, but with different rate constants) had to be invoked. We argued that, to a good approximation, a single Poisson model could be assumed. However, the limits of this approximation should be kept in mind.

1. In Fig. 13, most of the variance between different collaterals was within the range of one and the same Poisson distribution. Nevertheless, there were more outliers than expected. This may reflect the fact that the overall density of synapses in the cortex is somewhat lower in layers V/VI (e.g. Wolff 1976; Schüz and Palm 1989). It may also indicate that some pyramidal neurons tend to have higher or lower overall densities of synapses than others beyond the level of chance.

2. Figure 13 suggests also that the density of swellings λ may be somewhat larger for long collaterals than for short ones. The interpretation of this observation depends on the true length of the 'short' collaterals. This is not always obvious: many collaterals referred to as 'short' are, in fact, the initial segments of collaterals of unknown length leaving the section. If most of the 'short' collaterals in Fig. 13 were truly short, this would suggest that the rate λ of the Poisson process is to some extent a function of the collateral length, with λ increasing slightly for longer collaterals. A tentative explanation for such lower numbers of swellings on short collaterals might be the following; short collaterals could be the remnants of axonal fibres which did not succeed in finding appropriate postsynaptic partners during the critical period and which were consequently pruned (Callaway and Katz 1990) to short lengths. If, on the other hand, many of the short collaterals in Fig. 13 were, in fact, the initial segments of long ones, this would indicate that synaptic swellings are somewhat less frequent in the vicinity of a proximal branching point, and that they become more dense as one proceeds in the distal direction. In other words, the rate λ of the Poisson process would slightly increase with increasing distance from the proximal branching point, i.e. the Poisson process would be rate-modulated.

Despite the phenomena described under (1) and (2), the deviation from a single Poisson distribution with constant rate parameter $\lambda = 0.22$ swellings/μm is actually quite small. The large majority of collaterals in our sample is adequately described by a single Poisson model.

We should emphasize that our analysis focused on the one-dimensional distribution of synapses along axon collaterals. The stochastic nature of this distribution does not rule out the possibility of any preferences in three-dimensional cortical space. Three-dimensional clusters of high synaptic density have indeed been described (cat visual cortex: Gilbert and Wiesel 1983; cat auditory cortex: Ojima et al. 1991; monkey somatosensory cortex: DeFelipe et al. 1986; rat visual cortex: Lohmann 1992). In view of our results, however, one has to conclude that such discrete patches of high synaptic density correspond to peculiarities in the axonal branching patterns. Given that the synaptic load of axonal branches essentially follows a single Poisson distribution, the only way to ensure an increased density of synapses in a specific region in space is to send out a correspondingly higher number of axon branches into that region. Indeed, the three-dimensional clusters of high synaptic density, described in the studies quoted above, coincide with clusters of axonal ramifications. This is in good agreement with a study by Amir et al. (1993) on biocytin-stained axons in the monkey visual cortex. They showed that the average distance between swellings is very similar within and outside clusters of axonal branches. Such findings clearly suggest that it is worthwhile investigating the quantitative properties of axonal branching patterns and determining, for instance, the minimal requirements a probabilistic model would have to fulfill to describe such branching statistics adequately (Nelken 1992). Statistical analysis and model work along these lines are currently in progress in our laboratory (Leuchtenberg et al. 1993).

4.5 Conclusions with respect to cortical connectivity

One of the central issues in cortical anatomy is the nature of the rules that describe neuronal connectivity. Some formulate these rules as quasi-deterministic and highly specific (e.g. Hubel and Wiesel 1962; Lund and Boothe 1975; Kisvárday 1992), whereas others favour a probabilistic approach, i.e. one that is governed by chance (e.g. Sholl 1956; Cragg 1967; Peters and Feldman 1976;

Braitenberg 1978b; Abeles 1982, 1991). As far as the system of pyramidal cells is concerned, there is evidence for the view that deterministic rules do exist on a global level, with regard to the regions in which ramifications are made and to the general pattern of ramification, but that there is no detailed wiring prescription at the synaptic level, specifying the connectivity within a region of ramification. The results by DeFelipe et al. (1986) and others (e.g. Rockland and Lund 1983; Greilich 1984; Pandya and Yeterian 1985; Zeki and Shipp 1989) on long range connections provide evidence for specificity at the global level. The evidence for the synaptic level is somewhat ambiguous. Combined HRP-electron microscopic studies (Gabbott et al. 1987; McGuire et al 1991) and statistical investigations of the cortical neuropil (Sholl 1956; Cragg 1967; Braitenberg and Schüz 1991) support the assumption that the axons of pyramidal cells tend to make synapses with all possible targets within their reach. Some HRP-electron microscopic studies, however, provide evidence for a certain selectivity (McGuire et al. 1984; White and Keller 1987). Possibly, both kinds of connectivity exist in parallel or – which in our view is more likely–can be reconciled into a single, unified conception when a more adequate definition of the notion of 'possible targets' is available (for a more extensive discussion of this issue see White 1989; Schüz 1992). In any case, the results obtained for the pyramidal cells investigated in the present study support a probabilistic model of connectivity on the synaptic level.

Clearly, the present work is only concerned with the anatomical substrate of cortical connectivity. The efficacies of synapses and, hence, any possible differential organization in the spatial arrangement of these efficacies cannot be assessed by anatomical means. This applies even more so when the dynamic aspects of cortical connectivity are considered. Several such dynamics are, in fact, expected to play a role. First, and presumably on a relatively long time scale (of the order of minutes or more), there is the phenomenon of synaptic plasticity commonly associated with learning (Hebb 1949). Thus, it is quite conceivable that highly specific circuits may 'develop' on the background of random connectivity through a process of synaptic strengthening. Another source of coupling dynamics may shape the efficacy distribution on an even shorter time scale, from seconds down to the millisecond range. Such rapid modulations of neuronal coupling have, in fact, been observed in different cortical areas in the form of stimulus- and behaviour-related variations of coherence in the activities of simultaneously recorded neurons (e.g. Aertsen and Gerstein 1991; Vaadia and Aertsen 1992). Several different mechanisms may explain such rapid modifications, the most plausible one residing in the space-time dynamics of the network activity distribution (Aertsen and Preissl 1991). Neither of these dynamic modifications of cortical coupling is expected to show up in the anatomical connectivity distribution. Rather, this anatomical connectivity provides the structural substrate on which the various dynamics can 'flourish' and develop meaningful associations among the neurons. This enables the network to dynamically organize itself into functional groupings, depending on the instantaneous computational demands (Abeles 1991; Aertsen et al. 1994). In this context, it is interesting to note that the random nature of the local connectivity imposes minimal structural constraints on which neural associations may eventually evolve. Rather, the anatomy seems to guarantee that the available resource of synaptic connections can be utilized with the maximum degree of freedom.

Acknowledgements. We are grateful to Prof. Valentino Braitenberg, Prof. Moshe Abeles and Dr. Israel Nelken for enlightening discussions, to Monika Dortenmann for technical help, and to Shirley Würth for linguistic assistance. Financial support for this study was provided by the German Ministry for Science and Technology (BMFT).

References

Abeles M (1982) Local cortical circuits. Springer, Berlin Heidelberg New York

Abeles M (1991) Corticonics. Neural circuits of the cerebral cortex. Cambridge University Press, Cambridge, UK

Aertsen AMHJ, Gerstein GL (1991) Dynamic aspects of neuronal cooperativity: fast stimulus-locked modulations of 'effective connectivity'. In: Krüger J (ed) Neuronal cooperativity. Springer, Berlin Heidelberg New York, pp 52–67

Aertsen A, Preissl H (1991) Dynamics of activity and connectivity in physiological neuronal networks. In: Schuster H (ed) Nonlinear dynamics and neuronal networks. VCH, Weinheim

Aertsen A, Erb M, Palm G (1994) Dynamics of functional coupling in the cerebral cortex: an attempt at a model-based interpretation. Physica D (in press)

Amir Y, Harel M, Malach R (1993) Cortical hierarchy reflected in the organization of intrinsic connections in macaque monkey visual cortex. J Comp Neurol 334:19–46

Blue ME, Parnavelas JG (1983) The formation and maturation of synapses in the visual cortex of the rat. II. Quantitative analysis. J Neurocytol 12:697–712

Braitenberg V (1978a) Cortical architectonics: general and areal. In: Brazier MAB, Petsche H (eds) Architectonics of the cerebral cortex. Raven Press, New York

Braitenberg V (1978b) Cell assemblies in the cerebral cortex. In: Heim R, Palm G (eds) Theoretical approaches to complex systems. (Lecture Notes in Biomathematics, vol 21). Springer, Berlin Heidelberg New York, pp 171–188

Braitenberg V, Schüz A (1991) Anatomy of the cortex. Statistics and geometry. Springer, Berlin Heidelberg New York

Callaway EM, Katz LC (1990) Emergence and refinement of clustered horizontal connections in cat striate cortex. J Neurosci 10: 1134–1153

Colonnier M (1964) The tangential organization of the visual cortex. J Anat 98:327–344

Cox DR, Lewis PAW (1966) The statistical analysis of series of events. Methuen, London

Cragg BG (1967) The density of synapses and neurones in the motor and visual areas of the cerebral cortex. J Anat 101:639–654

DeFelipe J, Fairén A (1988) Synaptic connections of an interneuron with axonal arcades in the cat visual cortex. J Neurocytol 17: 313–323

DeFelipe J, Conley M, Jones EG (1986) Long-range focal collateralization of axons arising from corticocortical cells in monkey sensory-motor cortex. J Neurosci 6:3749–3766

Feller W (1957) An introduction to probability theory and its applications. Wiley, New York

Foh E, Haug H, König M, Rast A (1973) Quantitative Bestimmung zum feineren Aufbau der Sehrinde der Katze, zugleich ein methodischer Beitrag zur Messung des Neuropils. Microsc Acta 75:148–168

Freund TF, Martin KAC, Smith AD, Somogyi P (1983) Glutamate decarboxylase-immunoreactive terminals of Golgi-impregnated axoaxonic cells and of presumed basket cells in synaptic contact with pyramidal neurons of the cat's visual cortex. J Comp Neurol 221:263–278

Gabbott PLA, Martin KAC, Whitteridge D (1987) Connections between pyramidal neurons in layer 5 of cat visual cortex (area 17). J Comp Neurol 259:364–381

Gilbert CD, Wiesel TN (1983) Clustered intrinsic connections in cat visual cortex. J Neurosci 3:1116–1133

Glaser EM, Ruchkin DS (1976) Principles of neurobiological signal analysis. Academic Press, New York

Greilich H (1984) Quantitative Analyse der cortico-corticalen Fernverbindungen bei der Maus. Thesis, University of Tübingen

Hebb D (1949) The organization of behavior. A neuropsychological theory. Wiley, New York

Hellwig B (1992) Dichte und Verteilung präsynaptischer Boutons auf Golgi-gefärbten Axonen. Ein Beitrag zur Synaptologie der Großhirnrinde. Thesis, University of Tübingen

Hellwig B, Schüz A (1989) Density and distribution of presynaptic boutons on Golgi-stained axons in the cerebral cortex of the mouse. In: Elsner N, Singer W (eds) Dynamics and plasticity in neuronal systems. Proceedings of the 17th Göttingen Neurobiology Conference. Thieme, Stuttgart

Hubel DH, Wiesel TN (1962) Receptive fields, binocular interaction and functional architecture in the cat's visual cortex. J Physiol 160:106–154

Kisvárday ZF (1992) An example for specific connections in the visual cortex. In: Aertsen A, Braitenberg V (eds) Information processing in the cortex. Experiments and theory. Springer, Berlin, Heidelberg New York, pp 23–27

Kisvárday ZF, Martin KAC, Freund TF, Maglóczky ZF, Whitteridge D, Somogyi P (1986) Synaptic targets of HRP-filled layer III pyramidal cells in the cat striate cortex. Exp Brain Res 64:541–552

Kisvárday ZF, Martin KAC, Friedlander MJ, Somogyi P (1987) Evidence for interlaminar inhibitory circuits in the striate cortex of the cat. J Comp Neurol 260:1–19

Leuchtenberg P, Aertsen A, Lohmann H, Nelken I (1993) A stochastical model of axonal branching patterns in the cortex. In: Elsner N, Heisenberg M (eds) Gene-brain-behaviour. Proceedings of the 21st Göttingen Neurobiology Conference. Thieme, Stuttgart, p 474

Lohmann H (1992) Axon collaterals of pyramidal cells in extrastriate visual cortex of the rat. In: Elsner N, Richter DW (eds) Rhythmogenesis in neurons and networks. Thieme, Stuttgart, p 348

Lund JS, Boothe RG (1975) Interlaminar connections and pyramidal neuron organisation in the visual cortex, area 17, of the macaque monkey. J Comp Neurol 159:305–334

Martin KAC, Whitteridge D (1984) Form, function and intracortical projections of spiny neurones in the striate visual cortex of the cat. J Physiol (Lond) 353:463–504

Matthews DA, Cotman C, Lynch G (1976) An electron microscopic study of lesion-induced synaptogenesis in the dentate gyrus of the adult rat. II. Reappearance of morphologically normal synaptic contacts. Brain Res 115:23–31

McGuire BA, Hornung JP, Gilbert CD, Wiesel TN (1984) Patterns of synaptic input to layer 4 of cat striate cortex. J Neurosci 4:3021–3033

McGuire BA, Gilbert CD, Rivlin PK, Wiesel TN (1991) Targets of horizontal connections in macaque primary visual cortex. J Comp Neurol 305:370–392

Nelken I (1992) A probabilistic approach to the analysis of propagation delays in large cortical axon trees. In: Aertsen A, Braitenberg V (eds) Information processing in the cortex. Experiments and theory. Springer, Berlin Heidelberg New York, pp 29–49

Ojima H, Honda CN, Jones EG (1991) Patterns of axon collateralization of identified supragranular pyramidal neurons in the cat auditory cortex. Cerebral Cortex 1:80–94

Pandya DN, Yeterian EH (1985) Architecture and connections of cortical association areas. In: Peters A, Jones EG (eds) Cerebral cortex. Association and auditory cortices. Plenum Press, New York, pp 3–61

Peters A (1970) The fixation of central nervous tissue and the analysis of electron micrographs of the neuropil, with special reference to the cerebral cortex. In: Nauta WJH, Ebbesson SOE (eds) Contemporary research methods in neuroanatomy. Springer, Berlin Heidelberg New York, pp 56–76

Peters A, Feldman ML (1976) The projection of the lateral geniculate nucleus to area 17 of the rat cerebral cortex. I. General description. J Neurocytol 5:63–84

Peters A, Jones EG (1984) Classification of cortical neurons. In: Peter A, Jones EG (eds) Cerebral cortex, Vol I Cellular components of the cerebral cortex. Plenum Press, New York, pp 107–121

Peters A, Proskauer CC (1980) Synaptic relationships between a multipolar stellate cell and a pyramidal neuron in the rat visual cortex. A combined Golgi-electron microscope study. J Neurocytol 9:163–183

Ramón y Cajal S (1911) Histologie du Système Nerveux de l'Homme et des Vertébrés, (translated by L. Azoulay). Consejo superior de investigaciones cientificas, Instituto Ramón y Cajal, Madrid, 1972

Rockland KS, Lund JS (1983) Intrinsic laminar lattice connections in primate visual cortex. J Comp Neurol 216:303–318

Schüz A (1989) Untersuchungen zur Verknüpfungsstruktur der Großhirnrinde. Quantitative Studien am Cortex der Maus. Thesis, University of Tübingen

Schüz A (1992) Randomness and constraints in the cortical neuropil. In: Aertsen A, Braitenberg V (eds) Information processing in the cortex. Experiments and theory. Springer, Berlin Heidelberg New York, pp 3–21

Schüz A, Münster A (1985) Synaptic density on the axonal tree of a pyramidal cell in the cortex of the mouse. Neuroscience 15:33–39

Schüz A, Palm G (1989) Density of neurons and synapses in the cerebral cortex of the mouse. J Comp Neurol 286:442–455

Sholl DA (1956) The organization of the cerebral cortex. Wiley, New York

Somogyi P (1978) The study of Golgi stained cells and experimental degeneration under the electron microscope: a direct method for the identification in the visual cortex of three successive links in a neuron chain. Neuroscience 3:167–180

Somogyi P, Cowey A (1981) Combined Golgi and electron microscopic study on the synapses formed by double bouquet cells in the visual cortex of the cat and monkey. J Comp Neurol 195:547–566

Somogyi P, Hodgson AJ, Smith AD (1979) An approach to tracing neuron networks in the cerebral cortex and basal ganglia. A combination of Golgi staining, retrograde transport of horseradish peroxidase and anterograde degeneration of synaptic boutons in the same material. Neuroscience 4:1805–1852

Somogyi P, Nunzi MG, Gorio A, Smith AD (1983a) A new type of specific interneuron in the monkey hippocampus forming synapses exclusively with the axon initial segments of pyramidal cells. Brain Res 259:137–142

Somogyi P, Kisvárday ZF, Martin KAC, Whitteridge D (1983b) Synaptic connections of morphologically identified and physiologically characterized large basket cells in the striate cortex of cat. Neuroscience 10:261–294

Vaadia E, Aertsen A (1992) Coding and computation in the cortex: single-neuron activity and cooperative phenomena. In: Aertsen A, Braitenberg V (eds) Information processing in the cortex. Experiments and theory. Springer, Berlin Heidelberg New York, pp 81–121

Valverde F (1970) The Golgi method. A tool for comparative structural analysis. In: Nauta WJH, Ebbesson SOE (eds) Contemporary research methods in neuroanatomy. Springer, Berlin Heidelberg New York

Vrensen G, de Groot D (1975) The effect of monocular deprivation on synaptic terminals in the visual cortex of rabbits. A quantitative electron microscopic study. Brain Res 93:15–24

White EL (1989) Cortical circuits. Synaptic organization of the cerebral cortex. Structure, function, and theory. Birkhäuser, Boston

White EL, Hersch SM (1981) Thalamocortical synapses of pyramidal cells which project from SmI to MsI in the mouse. J Comp Neurol 198:167–181

White EL, Keller A (1987) Intrinsic circuitry involving the local axon collaterals of corticothalamic projection cells in mouse SmI cortex. J Comp Neurol 262:13–26

Winfield DA, Brooke RNL, Sloper JJ, Powell TPS (1981) A combined Golgi-electron microscopic study of the synapses made by the proximal axon and recurrent collaterals of a pyramidal cell in the somatic sensory cortex of the monkey. Neuroscience 6:1217–1230

Wolff JR (1976) Quantitative analysis of topography and development of synapses in the visual cortex. Exp Brain Res [Suppl] 1:259–263

Zeki S, Shipp S (1989) Modular connections between areas V2 and V4 of macaque monkey visual cortex. Eur J Neurosci 1:494–506